Utilisation de l'optimisation de forme pour la détermination de trajectoires de lasage

Thèse financée par le projet SOFIA

Mathilde Boissier[1,2], Grégoire Allaire[1], Christophe Tournier[2]

[1] CMAP, Ecole Polytechnique, France
[2] LURPA, ENS Paris Saclay, France

27/02/2020

Introduction

The LPBF process

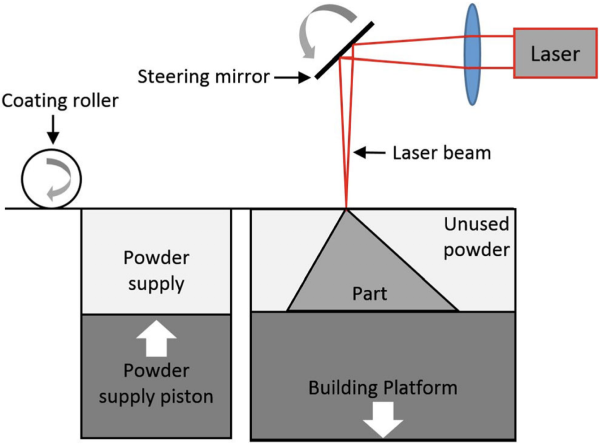

Process description (Bikas, Stavropoulos, and Chryssolouris (2016))

Laser path

State of the art : (Ding et al. (2015) and Liu et al. (2018))

parallel

contour

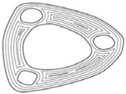

spiral

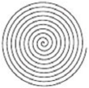

continuous

Medial Axis Transformation

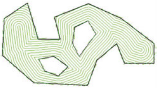

- Allocation of these paths to domain cells,
- Velocity and power optimization,
- "Live" path adaptation.

Goal :

- **path optimization "from scratch" (Alam, Nicaise, and Paquet (2019)),**
- **determination of "good paths" criteria,**
- **determination of shape constraints inducing good paths.**

LPBF modelization

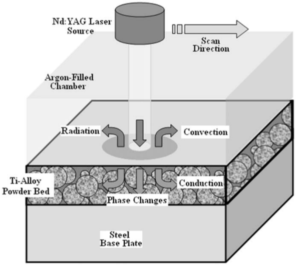

LPBF process
(Roberts et al. (2009))

Microscopic scale
(Megahed et al. (2016) and DebRoy et al. (2018))

- accurate model for the change of state, melting pool,
- 4 states considered: powder, solid, liquid, gaz.

Macrocospic scale
(Van Belle (2013), Megahed et al. (2016), and G. Allaire and Jakabčin (2018))

- conduction, convection and radiation
- 2 states considered: powder and solid.

Stakes at a macroscopic scale:

- **thermomechanics**: thermal expansion, residual stresses, solidification of the layer,
- **kinematics**: minimal execution time, easy to create.

Macroscopic 2D model (in the layer plane)

Heat equation (conduction only):

$$\begin{cases} \rho_{pow}.c_{p,pow}.\partial_t T - \nabla \cdot (\lambda_{pow}.\nabla T) + \frac{\lambda_{sol}}{L\Delta Z} T = \frac{Q}{L}, & (t,x) \in (0,t_F) \times D, \\ \lambda_{pow}.\nabla T \cdot n = 0, & (t,x) \in (0,t_F) \times \partial D, \\ T(0,x) = T_{init}(x) & x \in D. \end{cases}$$

Source model: $Q(t,x) = P \exp\left(-\delta |x - u(t)|^2\right)$, ($u(t)$ the laser path).

Physical characteristics time independent (powder or solid value chosen depending on the context).

Constraints to satisfy:

- change of state: $\forall x \in D, \exists t \quad \text{such that} \quad T(t,x) > T_\Phi$,
- thermal expansion: $\forall x \in D, \forall t, \quad T(t,x) < T_M$,
- ~~residual stresses.~~

Outline

SOFIA CMAP LURPA

Steady problem

Optimization problem to consider (Boissier, Allaire, and Tournier (2019))

Steady model: source on the whole trajectory at the same time (heating thread).

Objective : vary the path Γ in order to minimize its length ($J(\Gamma)$) while satisfying the change of phase (C_Φ) and maximal temperature constraints (C_M).

$$\min_{\Gamma} J(\Gamma) = \int_{\Gamma} ds$$

while satisfying the constraints

$$\begin{cases} C_{\Phi,st} = \int_D \left[(T_\Phi - T)^+\right]^2 dx = 0 & (T > T_\Phi), \\ C_{M,st} = \int_D \left[(T - T_M)^+\right]^2 dx = 0 & (T < T_M). \end{cases}$$

and T solution of:

$$\begin{cases} -\nabla \cdot (\lambda_{pow.} \nabla T) + \frac{\lambda_{sol.}}{L\Delta Z} T = \frac{P}{L} \chi_\Gamma, & (t,x) \in (0,t_F) \times D \\ \lambda_{pow.} \nabla T \cdot n = 0 & (t,x) \in (0,t_F) \times \partial D \end{cases}$$

Computation of the speed of variation: shape optimization (Henrot and Pierre (2018) and G. Allaire, Jouve, and Toader (2004))

Shape optimization: variation with respect to a vector field ϑ,

Γ regular curve with chosen orientation, which tangent is τ, which normal is n and curvature κ with A and B its endpoints.

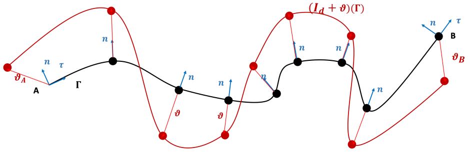

- Shape derivative of $J(\Gamma) = \int_\Gamma f(s)ds$:

$$J'(\Gamma)(\vartheta) = \int_\Gamma [\partial_n f + \kappa f]\, \vartheta \cdot n ds + f(B)\vartheta(B)\cdot\tau(B) - f(A)\vartheta(A)\cdot\tau(A)$$

- Then:

$$J(\Gamma^{n+1}) = J(\Gamma^n) + J'(\Gamma^n)(\vartheta) + o(\vartheta)$$

and ϑ is chosen such that $J(\Gamma^{n+1}) \leq J(\Gamma^n)$.

Numerical adaptation, steady problem

Line modelling: front tracking methods (Tryggvason et al. (2001))

Path discretization without modifying the mesh used for heat equation.

- control the curve's discretization and approximate continuous values (normal, curvature, ...),
- communicate between the discretization and the mesh.

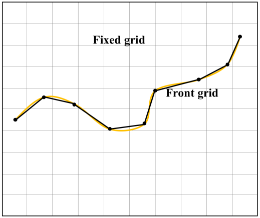

Algorithm

1. initial guess,
2. computation of the objective and constraints functions (heat equation),
3. computation of the shape derivative,
4. advection of the path and control of the its discretization,
5. computation of the objective and constraints functions (heat equation),
6. **if improvement: iteration accepted** back to 3.
7. **else: iteration refused** the step is decreased and back to 4.

Simple results

Values: (G. Allaire and Jakabčin (2018) and Van Belle (2013))
$D = 10cm \times 10cm, \quad \lambda_{sol.} = 15W.m^{-1}K^{-1}, \quad \lambda_{\mathbf{pow.}} = \mathbf{0.25W.m^{-1}K^{-1}}, \quad L = 10cm, \quad \Delta Z = 1m, \quad P = 800W.m^{-2}, \quad T_{\Phi} = 1700K, \quad \mathbf{T_M = 2000K}, \quad T_{init} = 500K.$

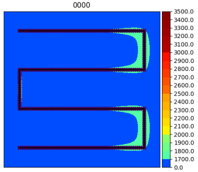

L = 1.01, $C_\phi = 1.03e^{-2}$, $C_{M,in} = 5.89e^{-2}$

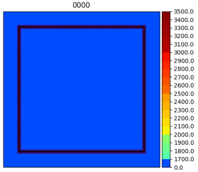

L = 1.03, $C_\phi = 1.20e^{-1}$, $C_{M,in} = 8.46e^{-2}$

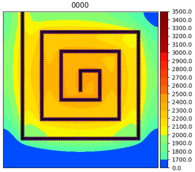

L = 1.01, $C_\phi = 1.15e^{-11}$, $C_{M,in} = 0$

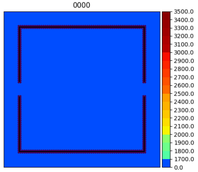

L = 1.03, $C_\phi = 1.08e^{-2}$, $C_{M,in} = 1.38e^{-2}$

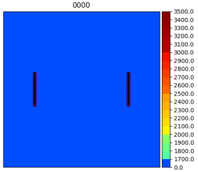

L = 1.03, $C_\phi = 2.86e^{-1}$, $C_{M,in} = 2.31e^{-1}$

Simple results

Values: (G. Allaire and Jakabčin (2018) and Van Belle (2013))
$D = 10cm \times 10cm$, $\lambda_{sol.} = 15W.m^{-1}K^{-1}$, $\lambda_{\mathbf{pow.}} = \mathbf{0.25W.m^{-1}K^{-1}}$, $L = 10cm$, $\Delta Z = 1m$, $P = 800W.m^{-2}$, $T_{\Phi} = 1700K$, $\mathbf{T_M = 2000K}$, $T_{init} = 500K$.

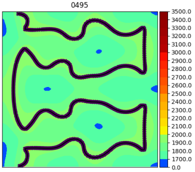

L = 1.01, $C_{\phi} = 1.03e^{-2}$,
$C_{M,in} = 5.89e^{-2}$

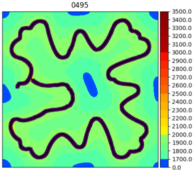

L = 1.03, $C_{\phi} = 1.20e^{-1}$,
$C_{M,in} = 8.46e^{-2}$

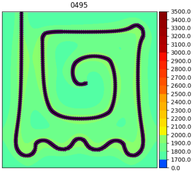

L = 1.01, $C_{\phi} = 1.15e^{-11}$,
$C_{M,in} = 0$

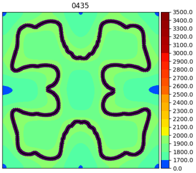

L = 1.03, $C_{\phi} = 1.08e^{-2}$,
$C_{M,in} = 1.38e^{-2}$

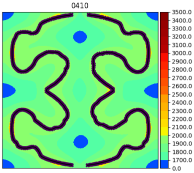

L = 1.03, $C_{\phi} = 2.86e^{-1}$,
$C_{M,in} = 2.31e^{-1}$

SOFIA CMAP LURPA

Influence of the maximum temperature and the powder conductivity

Values: (G. Allaire and Jakabčin (2018) and Van Belle (2013)) $D = 10cm \times 10cm$, $\lambda_{sol.} = 15W.m^{-1}K^{-1}$, $L = 10cm$, $\Delta Z = 1m$, $P = 800W.m^{-2}$, $T_\Phi = 1700K$, $T_{init} = 500K$.

Influence of the maximal temperature:

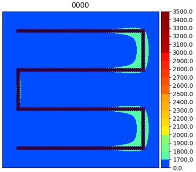

$T_{M,in} = 2000K$, $K_{pow.} = 0.25W.m^{-1}K^{-1}$

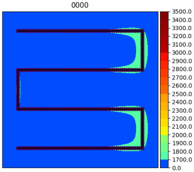

$T_{M,in} = 2500K$, $K_{pow.} = 0.25W.m^{-1}K^{-1}$

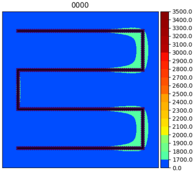

$T_{M,in} = 3000K$, $K_{pow.} = 0.25W.m^{-1}K^{-1}$

Influence of the conductivity:

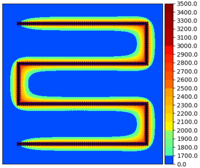

$T_{M,in} = 2000K$, $K_{pow.} = 0.025W.m^{-1}K^{-1}$

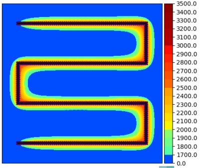

$T_{M,in} = 3000K$, $K_{pow.} = 0.025W.m^{-1}K^{-1}$

Influence of the maximum temperature and the powder conductivity

Values: (G. Allaire and Jakabčin (2018) and Van Belle (2013)) $D = 10cm \times 10cm$, $\lambda_{sol.} = 15W.m^{-1}K^{-1}$, $L = 10cm$, $\Delta Z = 1m$, $P = 800W.m^{-2}$, $T_{\Phi} = 1700K$, $T_{init} = 500K$.

Influence of the maximal temperature:

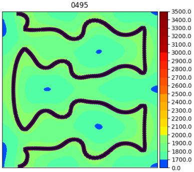

$T_{M,in} = 2000K$, $K_{pow.} = 0.25W.m^{-1}K^{-1}$

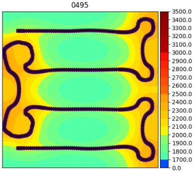

$T_{M,in} = 2500K$, $K_{pow.} = 0.25W.m^{-1}K^{-1}$

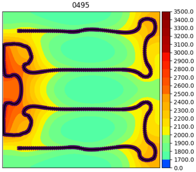

$T_{M,in} = 3000K$, $K_{pow.} = 0.25W.m^{-1}K^{-1}$

Influence of the conductivity:

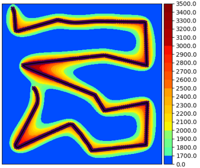

$T_{M,in} = 2000K$, $K_{pow.} = 0.025W.m^{-1}K^{-1}$

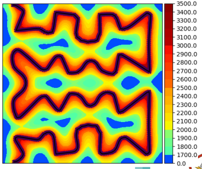

$T_{M,in} = 3000K$, $K_{pow.} = 0.025W.m^{-1}K^{-1}$

Building a fixed shape

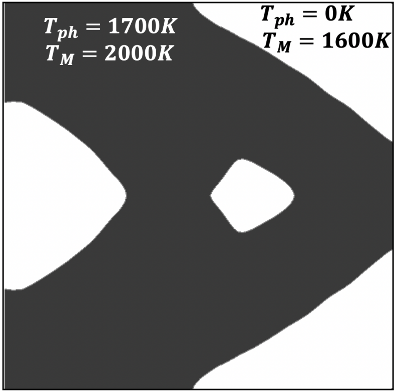

Building a fixed shape

Values: (G. Allaire and Jakabčin (2018) and Van Belle (2013)) $D = 10cm \times 10cm$, $\lambda_{sol.} = 15W.m^{-1}K^{-1}$, $L = 10cm$, $\Delta Z = 1m$, $P = 800W.m^{-2}$, $T_\Phi = 1700K$, $T_{init} = 500K$, $T_{M,out} = 1600K$.

Initialization A:

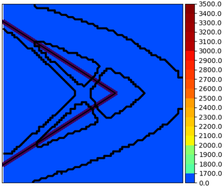

$T_{M,in} = 2000K$, $K_{pow.} = 0.25W.m^{-1}K^{-1}$

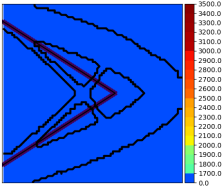

$T_{M,in} = 3000K$, $K_{pow.} = 0.25W.m^{-1}K^{-1}$

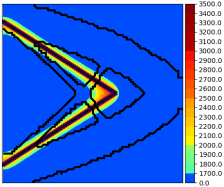

$T_{M,in} = 3000K$, $K_{pow.} = 0.025W.m^{-1}K^{-1}$

Initialization B:

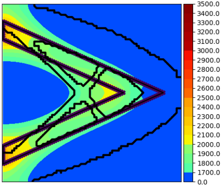

$T_{M,in} = 2000K$, $K_{pow.} = 0.25W.m^{-1}K^{-1}$

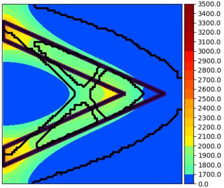

$T_{M,in} = 3000K$, $K_{pow.} = 0.25W.m^{-1}K^{-1}$

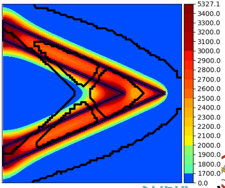

$T_{M,in} = 3000K$, $K_{pow.} = 0.025W.m^{-1}K^{-1}$

Building a fixed shape

Values: (G. Allaire and Jakabčin (2018) and Van Belle (2013)) $D = 10cm \times 10cm$, $\lambda_{sol.} = 15W.m^{-1}K^{-1}$, $L = 10cm$, $\Delta Z = 1m$, $P = 800W.m^{-2}$, $T_\Phi = 1700K$, $T_{init} = 500K$, $T_{M,out} = 1600K$.

Initialization A:

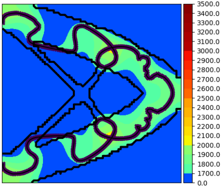

$T_{M,in} = 2000K$,
$K_{pow.} = 0.25W.m^{-1}K^{-1}$

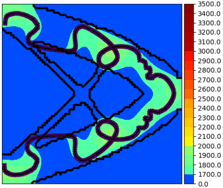

$T_{M,in} = 3000K$,
$K_{pow.} = 0.25W.m^{-1}K^{-1}$

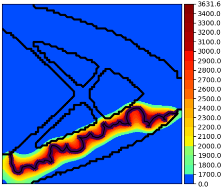

$T_{M,in} = 3000K$,
$K_{pow.} = 0.025W.m^{-1}K^{-1}$

Initialization B:

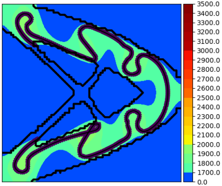

$T_{M,in} = 2000K$,
$K_{pow.} = 0.25W.m^{-1}K^{-1}$

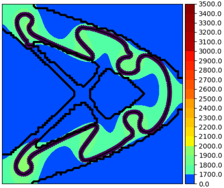

$T_{M,in} = 3000K$,
$K_{pow.} = 0.25W.m^{-1}K^{-1}$

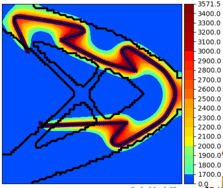

$T_{M,in} = 3000K$,
$K_{pow.} = 0.025W.m^{-1}K^{-1}$

Optimization problem

$$\min_\Omega J(\Omega) = \int_{\partial\Omega_N} g \cdot u ds$$
$$\text{such that } \int_\Omega dx = V_0$$

with $u \in H^1(\Omega)$ solution of

$$\begin{cases} -\mathrm{div}\,(Ae(u)) = 0 & \text{in } \Omega \\ Ae(u)\cdot n = g & \text{on } \partial\Omega_N \\ Ae(u)\cdot n = 0 & \text{on } \partial\Omega_F \\ u = 0 & \text{on } \partial\Omega_D \end{cases}$$

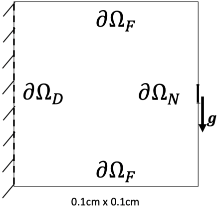

where A is Hooke's law.

Shape derivative: variation with respect to a vector field ϑ of Ω, a regular open domain with boundary $\partial\Omega$, which normal is n.

Shape derivative of $J(\Omega) = \int_\Omega f(s)ds$: $J'(\Omega)(\vartheta) = \int_{\partial\Omega} f\vartheta \cdot nds$

Shape optimization, results

$V_0 = 0.8 V_{ini}$

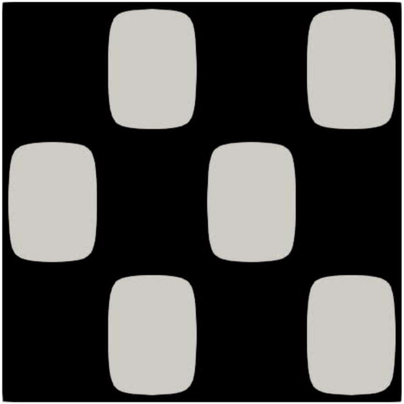

Shape optimization, results

$V_0 = 0.8\,V_{ini}$

Optimization problem

$$\min_{\Gamma,\Omega} \int_{\partial\Omega_N} g \cdot u ds + \int_\Gamma ds$$

$$\text{such that } \begin{cases} V = V_0 \\ T_\phi \leq T \leq T_M \end{cases}$$

with $T \in H^1(D)$ solution of

$$\begin{cases} -\nabla \cdot (\lambda_{pow.} \nabla T) + \frac{\lambda_{sol.}}{L\Delta Z} T = \frac{P}{L} \chi_\Gamma, & (t, x) \in (0, t_F) \times D \\ \lambda_{pow.} \nabla T \cdot n = 0 & (t, x) \in (0, t_F) \times \partial D \end{cases}$$

and $u \in H^1(\Omega)$ solution of

$$\begin{cases} -\mathrm{div}\,(Ae(u)) = 0 & \text{in } \Omega \\ Ae(u) \cdot n = g & \text{on } \partial\Omega_N \\ Ae(u) \cdot n = 0 & \text{on } \partial\Omega_F \\ u = 0 & \text{on } \partial\Omega_D \end{cases}$$

Results

Initialization A:

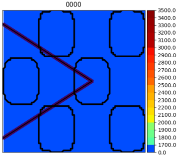

$T_{M,in} = 2000K$, $K_{pow.} = 0.25W.m^{-1}K^{-1}$

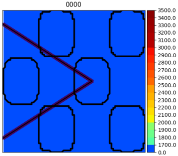

$T_{M,in} = 3000K$, $K_{pow.} = 0.25W.m^{-1}K^{-1}$

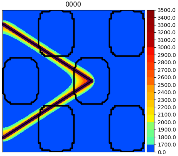

$T_{M,in} = 3000K$, $K_{pow.} = 0.025W.m^{-1}K^{-1}$

Initialization B:

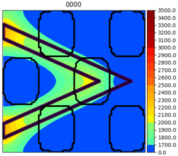

$T_{M,in} = 2000K$, $K_{pow.} = 0.25W.m^{-1}K^{-1}$

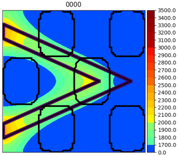

$T_{M,in} = 3000K$, $K_{pow.} = 0.25W.m^{-1}K^{-1}$

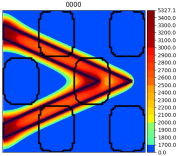

$T_{M,in} = 3000K$, $K_{pow.} = 0.025W.m^{-1}K^{-1}$

SOFIA CMAP LURPA

Results

Initialization A:

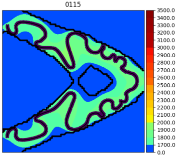

$T_{M,in} = 2000K$, $K_{pow.} = 0.25 W.m^{-1}K^{-1}$

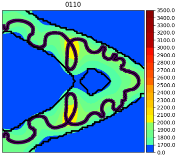

$T_{M,in} = 3000K$, $K_{pow.} = 0.25 W.m^{-1}K^{-1}$

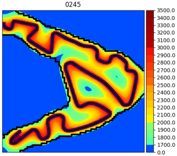

$T_{M,in} = 3000K$, $K_{pow.} = 0.025 W.m^{-1}K^{-1}$

Initialization B:

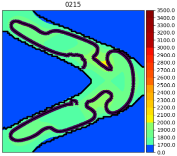

$T_{M,in} = 2000K$, $K_{pow.} = 0.25 W.m^{-1}K^{-1}$

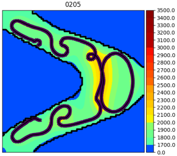

$T_{M,in} = 3000K$, $K_{pow.} = 0.25 W.m^{-1}K^{-1}$

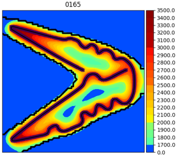

$T_{M,in} = 3000K$, $K_{pow.} = 0.025 W.m^{-1}K^{-1}$

SOFIA CMAP LURPA

Unsteady problem

Unsteady context (laser speed V fixed)

Objectives:

- final time: $L_g = t_F$
- change of state: $\forall x \in D, \exists t \in [0, t_F]$ such that $T(t,x) > T_\Phi$,

$$C_\Phi = \int_\Sigma \left[\left(T_\Phi - \max_t (|T(.,x)|) \right)^+ \right]^2 dx \approx \int_\Sigma \left[\left(T_\Phi - \|T(.,x)\|_{L^p(0,t_F)} \right)^+ \right]^2 dx.$$

- thermal expansion: $\forall (x,t) \in \Sigma \times [0, t_F],\ T(t,x) < T_M$,

$$C_M = \int_\Sigma \int_0^{t_F} \left[(T(t,x) - T_M)^+ \right]^2 dt dx.$$

Equations:

$$\begin{cases} \rho_{pow}.c_{p,pow}.\partial_t T - \nabla \cdot (\lambda_{pow}.\nabla T) + \frac{\lambda_{sol}}{L \Delta Z} T = \frac{Q(t,x)}{L}, & (t,x) \in (0, t_F) \times D, \\ \lambda_{pow}.\nabla T \cdot n = 0, & (t,x) \in (0, t_F) \times \partial D \\ T(0,x) = T_{init}(x) & x \in D. \end{cases}$$

with $Q(t,x) = P \exp\left(-\delta |x - u(t)|^2 \right)$

$$\begin{cases} \dot{u}(t) = V\tau(t) & t \in [t_1, t_F] \\ u(t_1) = \tilde{u}. \end{cases}$$

Optimal control of the line (Wendl, Pesch, and Rund (2010))

Control of the line: angle θ, formed by the horizontal and the tangent at each point.

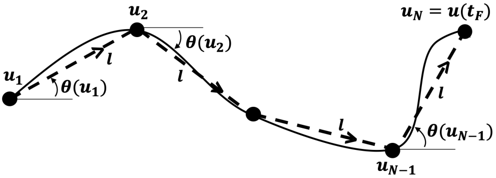

$$\min_{\theta, t_F, \tilde{u}} J = \Lambda_F(t_F) + \Lambda_\Phi(C_\Phi) + \Lambda_M(C_M),$$

while satisfying:

$$\begin{cases} \rho_{pow}.c_{p,pow}.\partial_t T - \nabla \cdot (\lambda_{pow}.\nabla T) + \frac{\lambda_{sol}}{L\Delta Z} T = \frac{Q(t,x)}{L}, & (t,x) \in (0, t_F) \times D, \\ \lambda_{pow}.\nabla T \cdot n = 0, & (t,x) \in (0, t_F) \times \partial D, \\ T(0,x) = T_{init}(x) & x \in D. \end{cases}$$

with $Q(t,x) = P \exp\left(-\delta |x - u(t)|^2\right)$, where the path equation u is given by:

$$\begin{cases} \dot{u}(t) = VF(\theta(t)) = V\left(\cos(\theta(t)), \sin(\theta(t))\right), & \forall t \in (t_1, t_F) \\ u(t_1) = \tilde{u} \end{cases}$$

SOFIA CMAP LURPA

Results:

Values: (not realistic but efficient to test the algorithm)

$\lambda_{sol.} = 10000 W.m^{-1}K^{-1}, \quad \lambda_{pow.} = 10000 W.m^{-1}K^{-1},$

$\rho_{sol.} = \rho_{pow.} = 8000 kg.m^{-3},$

$c_{sol.} = c_{pow.} = 450 J.kg^{-1}.K^{-1}$

$L = 10cm, \quad \Delta Z = 10cm, \quad P = 76800000 * (10^4) W.m^{-2},$

$T_\Phi = 773K, \quad T_{init} = 303K., \quad T_M = 2773, \quad p = 8.$

Phase constraint:

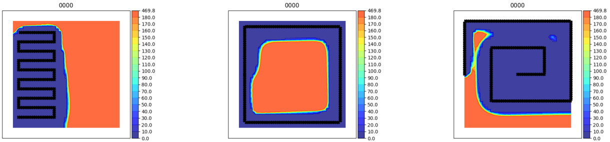

Max.temp. constraint:

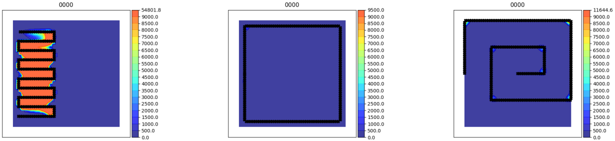

Results:

Values: (not realistic but efficient to test the algorithm)

$\lambda_{sol.} = 10000W.m^{-1}K^{-1}, \quad \lambda_{pow.} = 10000W.m^{-1}K^{-1},$
$\rho_{sol.} = \rho_{pow.} = 8000kg.m^{-3},$
$c_{sol.} = c_{pow.} = 450J.kg^{-1}.K^{-1}$
$L = 10cm, \quad \Delta Z = 10cm, \quad P = 76800000 * (10^4)W.m^{-2},$
$T_\Phi = 773K, \quad T_{init} = 303K., \quad T_M = 2773, \quad p = 8.$

Phase constraint:

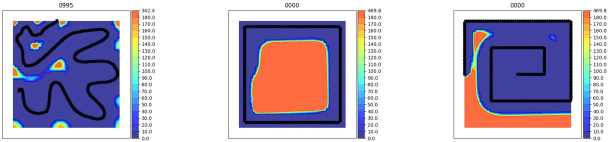

Max.temp. constraint:

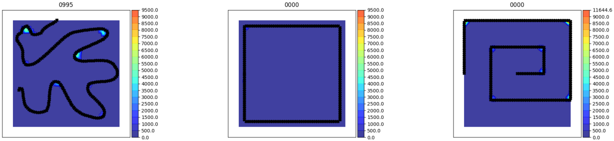

Results:

Values: (not realistic but efficient to test the algorithm)

$\lambda_{sol.} = 10000 W.m^{-1}K^{-1}, \quad \lambda_{pow.} = 10000 W.m^{-1}K^{-1},$
$\rho_{sol.} = \rho_{pow.} = 8000 kg.m^{-3},$
$c_{sol.} = c_{pow.} = 450 J.kg^{-1}.K^{-1}$
$L = 10cm, \quad \Delta Z = 10cm, \quad P = 76800000 * (10^4) W.m^{-2},$
$T_\Phi = 773K, \quad T_{init} = 303K., \quad T_M = 2773, \quad p = 8.$

Phase constraint:

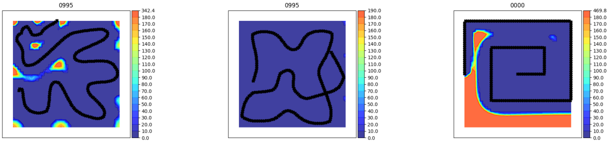

Max.temp. constraint:

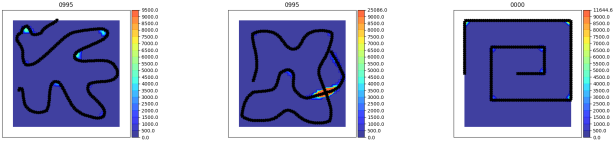

Results:

Values: (not realistic but efficient to test the algorithm)

$\lambda_{sol.} = 10000W.m^{-1}K^{-1}, \quad \lambda_{pow.} = 10000W.m^{-1}K^{-1},$
$\rho_{sol.} = \rho_{pow.} = 8000kg.m^{-3},$
$c_{sol.} = c_{pow.} = 450J.kg^{-1}.K^{-1}$
$L = 10cm, \quad \Delta Z = 10cm, \quad P = 76800000 * (10^4)W.m^{-2},$
$T_\Phi = 773K, \quad T_{init} = 303K., \quad T_M = 2773, \quad p = 8.$

Phase constraint:

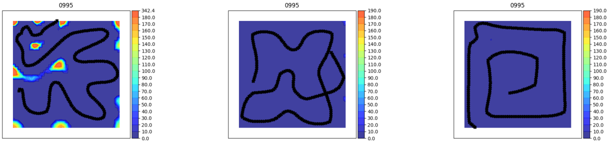

Max.temp. constraint:

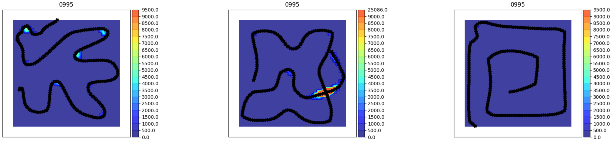

Conclusion and perspectives

Perspectives

Short terms perspectives:

- steady case:
  - allow for the splitting of the path and gathering many: topological derivative or power optimization with bounded variation constraints,
  - determine criteria for a "good path" and a "good shape".
- unsteady case:
  - improve the optimal control model,
  - allow for the splitting of the path and gathering many: topological derivative or power optimization with bounded variation constraints,
  - couple the shape and path optimization,
  - calibrate the model to get realistic results,
  - determine criteria for a "good path" and a "good shape".

Long term perspectives:

- adapt the curve meshing to the industrial requirements,
- adding more realistic constraints (geometrical, thermal et mechanical),
- make the 2D case evolve to a layer by layer 3D optimization.

References I

Alam, Tonia-Maria, Serge Nicaise, and Luc Paquet (2019). "An optimal control problem governed by heat equation with nonconvex constraints applied to selective laser melting process". In: **Hal preprint: https://hal.archives-ouvertes.fr/hal-02302403**.

Allaire, Grégoire and Lukas Jakabčin (2018). "Taking into Account Thermal Residual Stresses in Topology Optimization of Structures Built by Additive Manufacturing". In: **Mathematical Models and Methods in Applied Sciences** 28.12, pp. 2313–2366.

Allaire, Grégoire, François Jouve, and Anca-Maria Toader (2004). "Structural Optimization Using Sensitivity Analysis and a Level-Set Method". In: **Journal of Computational Physics** 194.1, pp. 363–393.

Bikas, H., P. Stavropoulos, and G. Chryssolouris (2016). "Additive Manufacturing Methods and Modelling Approaches: A Critical Review". In: **The International Journal of Advanced Manufacturing Technology** 83.1-4, pp. 389–405.

Boissier, Allaire, and Tournier (2019). "Scanning Path Optimization Using Shape Optimization Tools". In: **Hal preprint: https://hal.archives-ouvertes.fr/hal-02410481, to appear in SMO**.

DebRoy, T. et al. (Mar. 2018). "Additive Manufacturing of Metallic Components Process, Structure and Properties". In: **Progress in Materials Science** 92, pp. 112–224.

References II

- Ding, Donghong et al. (2015). "A practical path planning methodology for wire and arc additive manufacturing of thinwalled structures". In: **Robotic and Computer-Integrated Manufacturing** 34, pp. 8–19.
- Henrot, Antoine and Michel Pierre (2018). **Shape Variation and Optimization**. Vol. 28. EMS Tracts in Mathematics. European Mathematical Society (EMS), Zürich.
- Liu, Jikai et al. (June 2018). "Current and Future Trends in Topology Optimization for Additive Manufacturing". In: **Structural and Multidisciplinary Optimization** 57.6, pp. 2457–2483.
- Megahed, Mustafa et al. (Dec. 2016). "Metal Additive-Manufacturing Process and Residual Stress Modeling". In: **Integrating Materials and Manufacturing Innovation** 5.1, pp. 61–93.
- Roberts, I. A. et al. (Oct. 2009). "A Three-Dimensional Finite Element Analysis of the Temperature Field during Laser Melting of Metal Powders in Additive Layer Manufacturing". In: **International Journal of Machine Tools and Manufacture** 49.12-13, pp. 916–923.
- Tryggvason, G. et al. (2001). "A Front-Tracking Method for the Computations of Multiphase Flow". In: **Journal of Computational Physics** 169.2, pp. 708–759.
- Van Belle, Laurent (2013). "Analyse, Modélisation et Simulation de l'Apparition de Contraintes En Fusion Laser Métallique". PhD thesis.

References III

Wendl, S., H. J. Pesch, and A. Rund (2010). "On a State-Constrained PDE Optimal Control Problem Arising from ODE-PDE Optimal Control". In: ed. by Moritz Diehl et al., pp. 429–438.